

How can estimates of mangrove subtype distribution in Northwestern Madagascar be constrained through the use of Planet data and The Google Earth Engine Mangrove Mapping (GEEMMM)?

JiaYu Wu

Master's in Forestry at the University of British Columbia

Topical Mentor: Trevor Gareth Jones

Final Report

Date: 04/07/2023

Abstract:

In response to the growing concerns about mangrove deforestation, recent studies have used various remote sensing technology like satellite imagery to measure the mangrove extent. In this work, we investigated the mangrove distribution in Northwestern Madagascar by using fine spatial imagery with pixel size as small as 3m and compared it with the result of traditional method based on relatively coarser Landsat data. Mangroves are an essential biodiverse ecosystem found along tropical and subtropical intertidal beaches, providing critical goods and services to coastal communities, and supporting diverse organisms. However, anthropogenic activities have caused the loss of mangroves in Madagascar, necessitating a new mapping approach utilizing the fine spatial resolution map from Planet data to create a map with advanced detail. The quantitative result central to this work is the new multi-date map of the Tsimipaika-Ampasindava-Ambaro Bays (TAB) from 2020 to 2022, which provides advanced detail and direct comparison with the shift in local mangrove species. The classification maps are based on Random Forest and Maximum Likelihood algorithms, and all of them have an overall accuracy of over 85%. The dynamics of mangrove forests from 2020 to 2022 are quantified, with an 12.6% loss in closed-canopy mangroves, and an 24.1% loss in open-canopy mangroves I is overestimated. Limitations regarding the classification model are also found in this study, including the overestimation of open canopy mangroves caused by the shadow and the seashore in the base map. This result shows the potential of using fine resolution satellite imagery in supervised land cover classification, and the corresponding challenges raised by the smaller pixel size.

Keywords: PlanetScope; mangroves; remote sensing; Madagascar; dynamics; supervised classification

1. Introduction

Mangroves are widespread along tropical and subtropical intertidal beaches across the globe (Yancho et al., 2020). Mangrove environments are incredibly biodiverse and productive, contribute to minimizing climate change, and provide critical goods and services to coastal residents (Jones et al., 2016). They are home to a diverse range of organisms, including bacteria, fungi, and algae as well as invertebrates, birds, and mammals (Wilkie & Fortuna, 2003). Madagascar is home to 20% of the African mangroves, many of which have undergone or are starting to exhibit indications of substantial deterioration and deforestation (Benson et al., 2017). Over 20% of Madagascar's mangroves were destroyed between 1990 and 2014 to make way for more wood, charcoal, and areas for farming and aquaculture (Jones et al., 2014). The second-largest mangrove ecosystem in Madagascar is found in the Tsimipaika-Ampasindava-Ambaro Bays (TAB), which is located on the northwest side of the country (Jones et al., 2014). These bays have suffered substantially from anthropogenic damage (Jones et al., 2014). In this

research, I will develop a detailed map of the existing mangrove resources in TAB to assist local resource management.

Obtaining a thorough and well-organized map is one of the most crucial elements in creating a robust management system for mangrove ecosystems. The most recent map of mangroves covering Ambanja Bay and a portion of Ambaro Bay was created by the Google Earth Engine Mangrove Mapping (GEEMMM) in 2000, 2010, and 2020. The GEEMMM provides a simple method for tracking and mapping mangrove ecosystems anywhere on the planet using Landsat data with a 30m pixel size (Yancho et al., 2020). However, Landsat data lacks the greater spatial and temporal resolution that could be offered by the PlanetScope imagery, with pixel sizes as small as 3 m (Yancho et al., 2020). A new mapping is necessary to guarantee the correct and precise classification of the present local mangrove subtypes. To achieve that goal, we intended to create a new multi-date map from 2020 to 2022 that concentrated on the area of interest utilizing the fine spatial resolution map from Planet data, with each pixel size as small as 3 m. Then compare it to the classification map provided by GEEMMM in 2020 to evaluate the capability of using fine-resolution spatial data to run the mangrove subtype classification. Additionally, the planet multi-date map provides a direct comparison with the change in local mangrove distribution from 2020 to 2022.

It is necessary and beneficial to update the classification and recent coverage of multiple mangrove species since they all have unique physical characteristics and behavioral traits. For instance, the closed-canopy mangrove has a higher carbon stock than the open-canopy mangrove (Benson et al., 2017). By getting access to the most detailed assessment of the mangrove ecosystem, the local populations can manage the mangrove source more effectively to increase its sustainability, boost living conditions, and reduce anthropogenic stressors (Benson et al., 2017).

2. Data and Study Site Summary

2.1. Study Area Description:

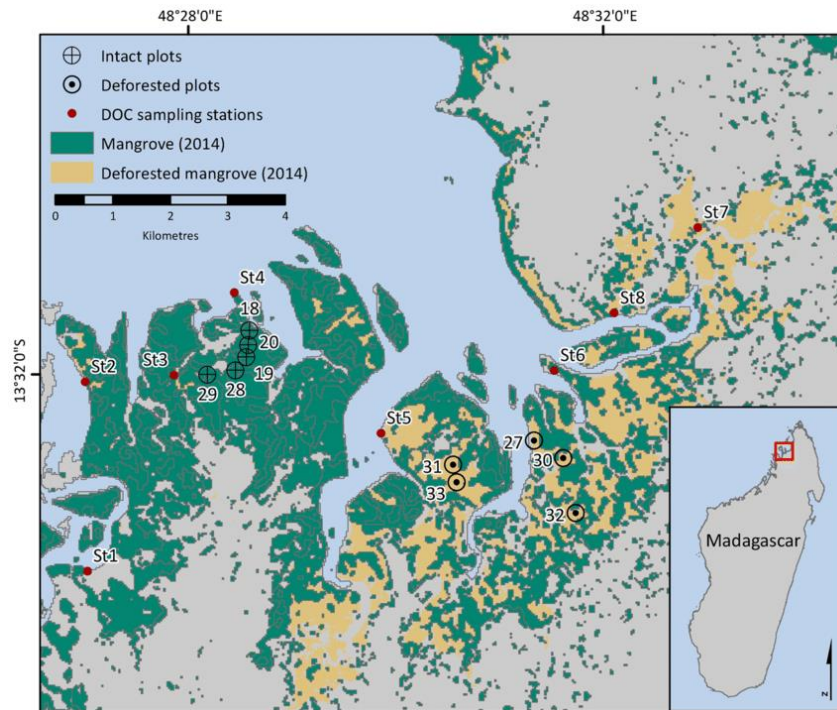


Figure 1 - Map of Tsimipaika Bay in northwest Madagascar with sampled plot locations in intact and deforested mangrove areas. St. labels are surface water sampling locations. (Arias-Ortiz et al., 2020)

Madagascar, the fifth-largest island in the world with 144 million acres, is located off the east coast of Africa (World Wildlife Fund, 2022). Madagascar has a tropical climate near its coast, a moderate temperature inland, and an arid environment in the south (World Wildlife Fund, 2022). Rich tropical rainforests, tropical dry forests, hills, and deserts may all be found on the island. The Western Indian Ocean is home to some of the largest coral reef systems and most extensive mangrove regions in the world, and it has more than 3,000 miles of coastline and more than 250 islands (World Wildlife Fund, 2022). Numerous creatures live in mangroves, including insects, birds, and mammals as well as bacteria, fungi, and algae (Wilkie & Fortuna, 2003). Additionally, mangroves can prevent erosion along the beach (Benson et al., 2017).

Over 20% of Madagascar's mangroves were destroyed between 1990 and 2014 to make way for more wood, charcoal, and areas for farming and aquaculture (Jones et al., 2014). The second-largest mangrove ecosystem in Madagascar is found in the Tsimipaika-Ampasindava-Ambaro Bays (TAB), which are in the country's northwest, and these bays have suffered substantially from anthropogenic damage (Jones et al., 2014).

2.2. Study Area Map:

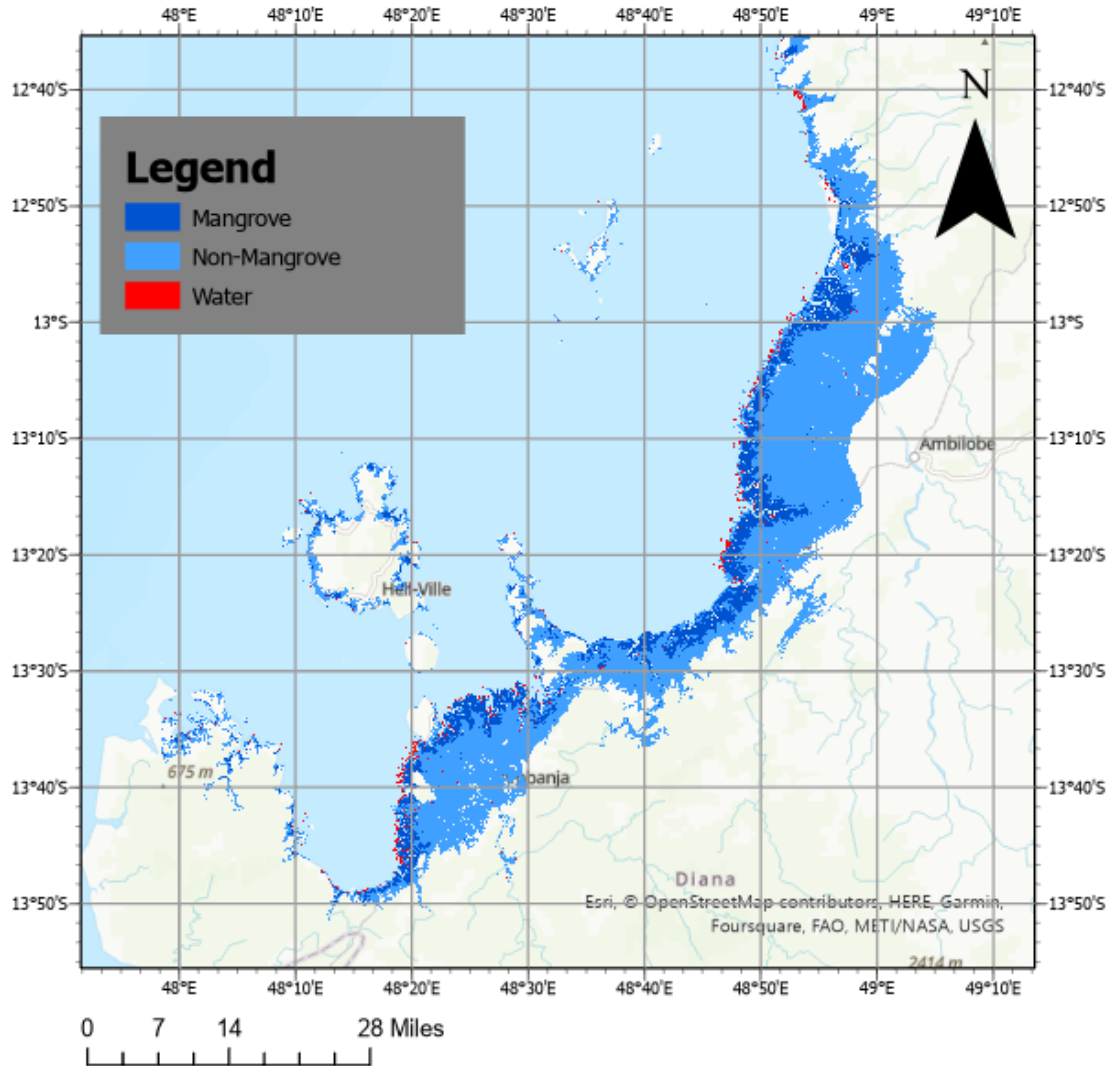


Figure 2 - The map with the Binary classification of Mangroves in Northwestern Madagascar in 2020 provided by GEEMMM

2.3. Data summary:

2.3.1. The Google Earth Engine Mangrove Mapping Methodology (GEEMMM) data

The Google Earth Engine Mangrove Mapping Methodology (GEEMMM) outcome for Augusts 2000, 2010, 2016, and 2020 are provided by the topical mentor. The GEEMMM offers a simple method for tracking and mapping mangrove ecosystems wherever they are found on the planet (Yancho et al., 2020). The datasets show the mangrove classifications in TAB, while the datasets have the coordinate of Longitude: 47.974887E to 49.110807E, and Latitude: 13.952274S to 12.562490S. GEEMMM is based on Landsat 8 data with a 30m x 30m pixel size (Yancho et al., 2020). Six bands are used in the classification of mangroves: Visible, NIR, and

SWIR bands (Yancho et al., 2020). Moreover, the classification is made by the interpretation of the Modified normalized difference water index (MNDWI), combined mangrove recognition index (CMRI), Modular mangrove recognition index (MMRI), Enhanced vegetation index (EVI), and Land Surface Water Index (LSWI) (Yancho et al., 2020).

2.3.2 The Planet data

The Planet data for 8/23/2016 and 8/4/2020 are retrieved from:

<https://www.planet.com/explorer>, which is accessed via the license of UBC Library – General Use, the data from 06/09/2020 to 08/04/2022 are collected by PlanetScope with a 3m pixel size. With a daily collection capability of 200 million km²/day, PlanetScope, operated by Planet, is a constellation of about 130 satellites that can picture the entire surface of the Earth every day with a Sun-synchronous Orbit (Planet, 2022). The coordinate of the datasets is also set to Longitude 47.974887E to 49.110807E and Latitude: 13.952274S to 12.562490S to match the GEEMMM map. PlanetScope provides spatial data with an accuracy of less than 10 m RMSE at the 90th percentile (Planet, 2022). Moreover, the two datasets used for this research are produced by the PSScene instrument of PlanetScope, which has the sensor type of a four-band frame imager with a butcher-block filter providing blue, green, red, and NIR stripes (Planet, 2022).

2.4. Data Summary Figures and Tables:

	Terrestrial Forest	Mixed Vegetation - Dry	Barren / Exposed	Residual Water	Closed-Canopy Mangrove	Open-Canopy Mangrove I	Open-Canopy Mangrove II	Mixed Vegetation - Healthy	Mixed Vegetation - Wet/Urban
Terrestrial Forest	68	0	0	0	0	0	0	0	0
Mixed Vegetation - Dry	0	55	0	0	0	0	0	0	0
Barren / Exposed	0	0	38	0	0	0	0	0	0
Residual Water	0	0	0	75	0	0	0	0	0
Closed-Canopy Mangrove	0	0	0	0	105	0	0	0	0
Open-Canopy Mangrove I	0	0	0	0	0	65	0	0	0
Open-Canopy Mangrove II	0	0	0	0	0	0	36	0	0

Mixed Vegetation - Healthy	0	0	0	0	0	0	0	37	0
Mixed Vegetation -									
Wet/Urban	0	0	0	0	0	0	0	0	79

Overall Accuracy: 1

Table 1-The accuracy of the full classification of mangroves at TAB in 2020, provided by GEEMMM.

The full classification of Mangroves in Northwestern Madagascar in 2020

-provided by the Google Earth Engine Mangrove Mapping Methodology

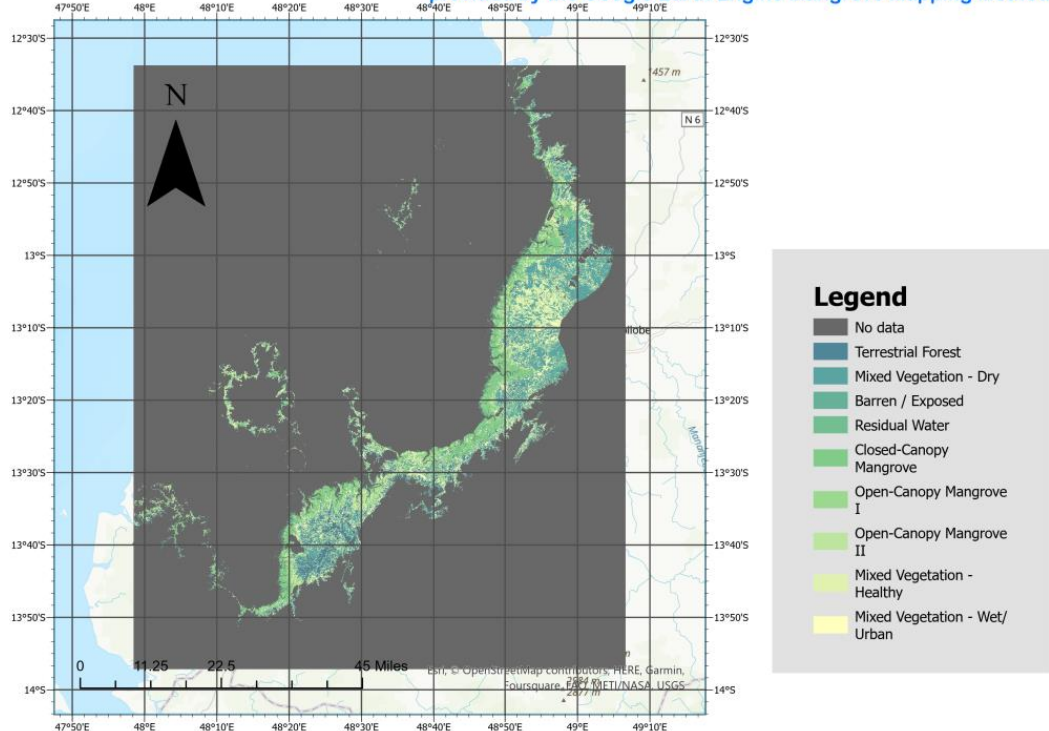


Figure 3- The map with the full classification of Mangroves in Northwestern Madagascar in 2020 provided by GEEMMM (Note: No data means GEEMMM automatically ignores the data outside the mangrove ecosystem inside the Area of Interest, known as AOI, so No data is assigned to deep grey color to mark the border of AOI)

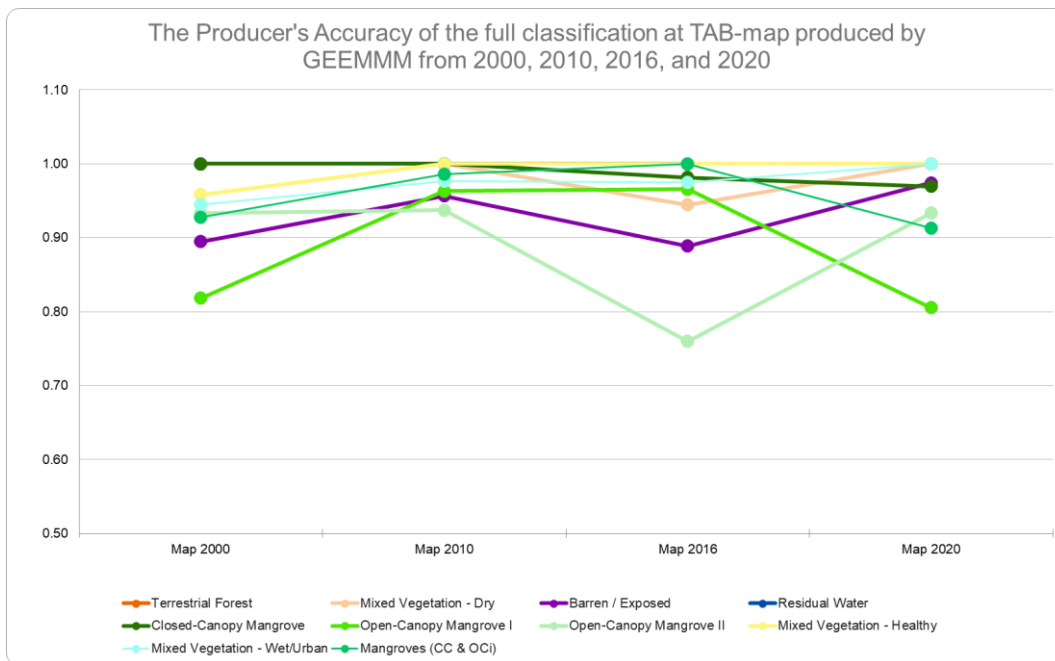


Figure 4- The Producer's Accuracy of the full classification at TAB-produced by GEEMMM from 2000, 2010, 2016, and 2020

3. Methods

To make a direct comparison between the classification result given by Planet data with the Google Earth Engine Mangrove Mapping Methodology (GEEMMM), I performed the supervised classification on multi-date maps of Planet data with a similar method used in GEEMMM as outlined in Yancho et al., 2020 as the modules below.

Module 1 – Defining the Area of Interest (AOI) and Compositing Imagery

1.1 Define the AOI and Acquire necessary Planet data

Several studies have shown the value of lowering the categorization extends to the bare minimum region because it lessens spectral confusion caused by extraneous scene elements (Giri et al., 2010, Jones et al., 2016). Previous research used 7 km as the buffer interval along the coastline based on covers the whole area of Ambanja-Ambaro Bays (AAB) including marine and terrestrial mangroves (Jones et al., 2016) Since current studies are all mapping based on relatively coarse data, i.e., Landsat 7 or 8 data, I enlarged the AOI to buffer interval of 15km along the coastline to make sure that all the possible areas available for mangrove growth are properly mapped. This ROI is used to specify the classification and dynamics extent, build image composites, and clip composite images and masks (such as elevation, slope, and water) (Yancho et al., 2020).

The purpose of accessing Planet data is to generate multi-date maps for 2020 and 2022. Then, a comprehensive web search will be conducted to locate all Planet data for TAB that spanned one or more dates between June 2020 and August 2022. Here, Planet data from August are the most optimistic since the GEEMMM maps available are from August. Seasonal fluctuations may impact land vegetation next to mangroves, and atmospheric conditions might vary throughout the year; thus, the ability to target certain months is vital for producing excellent picture composites (Yancho et al., 2020). Moreover, to obtain the most accurate and clear spatial data, cloud cover higher than 30% will be filtered out (Yancho et al., 2020). Datasets were gathered from internet repositories where they were accessible.

1.2 Generate multi-date maps for AOI

Planet data explorer allows users to clip the search result to the AOI, so all data downloaded will be limited to the AOI, which saved us the time of filtering out unnecessary data. ArcGIS Pro is the main tool used for mosaicking all the acquired PlanetScope Imagerys together to build a smooth map with no seam line.

With masking, the classification's scope is further constrained. The GEEMMM integrates cloud, water, slope, and elevation masks to provide a finished AOI, in line with other mangrove mapping studies (Yancho et al., 2020). Cloud mask has been applied in Module 1 section 1.1, during data collection. The water mask is built upon $NDWI < 0$ (Gao, 1996), which is not as strong in GEEMMM because fine-resolution spatial data is inaccessible to SWIR spectral data hence no Modified Normalized Difference Water Index (MNDWI) data is accessible to build the water mask in this research (Yancho et al., 2020). In this study, the same slope and elevation will be applied to the AOI, which are elevation < 39 m above sea level and slope $< 16\%$ as in the Myanmar study in GEEMMM (Yancho et al., 2020). The output of this module includes three strictly masked multi-date maps based on Planet data from 2020 and 2022 covering TAB are prepared for the classification in the next module.

Index	Abbreviation	Calculation	Reference
<i>Normalized Difference Vegetation Index</i>	NDVI	$(NIR - Red)/(NIR + Red)$	Gandhi et al., 2015
<i>Normalized Difference Water Index</i>	NDWI	$(Green - NIR)/(Green + NIR)$	McFeeters, 2013
<i>Combined Mangrove Recognition Index</i>	CMRI	$NDVI - NDWI$	Gupta et al., 2018
<i>Soil-Adjusted Vegetation Index</i>	SAVI	$1.5*(NIR - Red)/(NIR + Red + 0.5)$	Huete, 1988

<i>Optimized Soil-Adjusted Vegetation Index</i>	OSAVI	$(\text{NIR} - \text{Red}) / (\text{NIR} + \text{Red} + 0.16)$	Fern et al., 2018
<i>Enhanced Vegetation Index</i>	EVI	$2.5 * ((\text{NIR} - \text{red}) / (\text{NIR} + 6 * \text{Red} - 7.5 * \text{Blue} + 1))$	Matsushita et al., 2007

Table 2 – Spectral Indices available with 4 bands in PlanetScope – Blue, Green, Red, and NIR. The bold Index is the mangrove-specific spectral Index (Yancho et al., 2020).

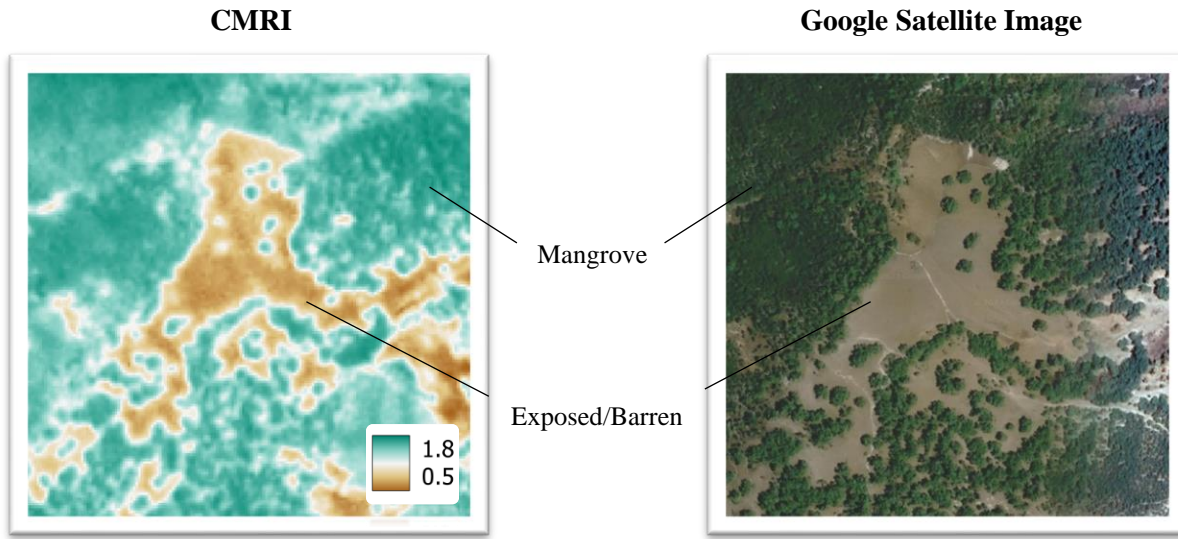


Figure 5- Example of the appearance of the only available Mangrove-specific spectral Index CMRI in identifying mangrove coverage with the comparison with Google Satellite map (Gupta et al., 2018).

Module 2 – Classification Reference Areas (CRAs), Spectral Separability, Classifications, and Accuracy Assessment

2.1 Derive CRAs for Planet data

For this study, by combining spectral indices and band combinations, I manually draw CRA polygons for 9 classes of landcover, while using the previous GEEMMM full classification result in 2020 at the same AOI as a reference. The number of CRAs used in the classification in 2020 and 2022 are listed below in Table 2, along with the property of different classes. The original CRAs used to generate the GEM maps represented 3x3 Landsat pixel (or 90 x 90 m) areas. Each of the new CRAs in this study will be a 3x3 Planet pixel neighborhood (i.e., 9 x 9 m). Also, to make sure I can make a direct comparison between the mangrove extent identified by the classification done by Planet data and GEEMMM, I also ran a simplified binary classification to specifically measure the extent of mangroves and non-mangroves as listed in Table 3 and compare the result with GEM.

Index	Class name	Description	2020	2022
--------------	-------------------	--------------------	-------------	-------------

1	Terrestrial Forest	Forests found on land with Canopy >30% closed	27	21
2	Mixed Vegetation – Dry	Grass; Shrub; Woodland; Inactive (senesced) Crops; some exposed soil + scattered trees (canopy <30%)	23	22
3	Barren / Exposed	Soil; Sediment; Sand; Rock; includes mudflats and recently deforested / burnt areas	25	25
4	Residual Water	Areas missed with water masking (includes water-logged mudflats - standing water)	11	11
5	Closed-Canopy Mangrove	Tall, mature stands; canopy >60% closed	35	34
6	Open-Canopy Mangrove I	Short-medium stands; canopy 30-60% closed; moderately influenced by background soil/mud	23	22
7	Open-Canopy Mangrove II	Stunted / short stands, shrub-dominant, very sparse; canopy 10-30% closed	16	16
8	Mixed Vegetation – Healthy	Grass; Shrub; Woodland; Active Crops; some exposed soil + scattered trees (canopy <30%)	24	18
9	Mixed Vegetation - Wet/Urban	Wet Farmlands; Swamps; Trees around streets/buildings	30	30
Total			214	199

Table 3- Index, class name, description, and numbers of Classification Reference Areas (CRAs) used in the 2020 and 2022 Full classification (Yancho et al., 2020).

Index	Class name	Description	2020	2022
1	Mangrove	Closed-Canopy Mangrove and Open-Canopy Mangrove I	116	55
2	Non-Mangrove	Terrestrial Forest, Mixed Vegetation, Barren/Exposed, Open-Canopy Mangrove II	179	134
3	Water	Areas missed with water masking (includes water-logged mudflats - standing water)	22	11
Total			317	200

Table 4- Index, class name, description, and numbers of Classification Reference Areas (CRAs) used in the 2020 and 2022 Binary classification.

2.2 Spectral Separability

Two charts are produced in this step to show the spectral parameters of four bands and nine classes of landcover. Using the minimum, maximum, and inter-quartile range for each band and each map class, the spectral parameters are extracted and summarized in a boxplot (Yancho et al., 2020). The second map is a line chart composed of the mean reflectance of classes in each band's mean wavelength to emphasize relationship between the band and reflectance of landcover.

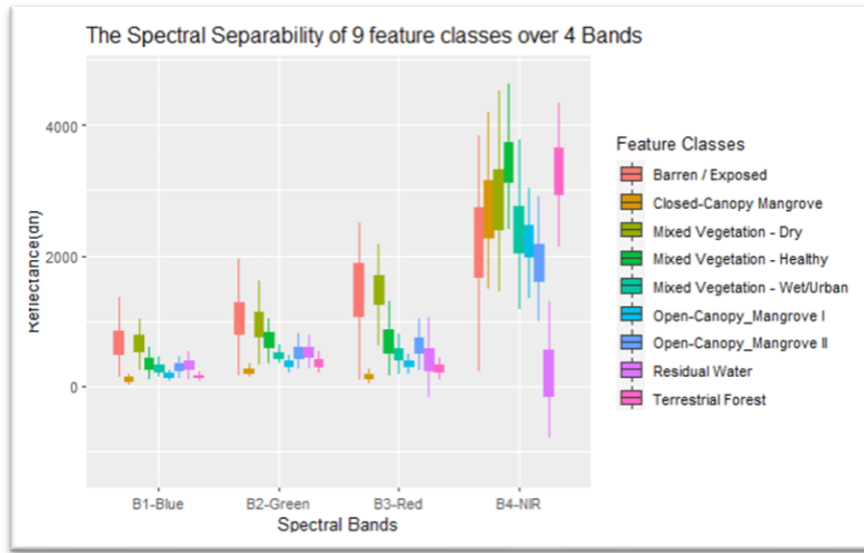


Figure 6 - The spectral separability of all target classes as represented by CRAs across PlanetScope Blue (B1), Green (B2), Red (B3), and NIR (B4) bands. The set of bar and whisker plots shows the min, max, and interquartile ranges.

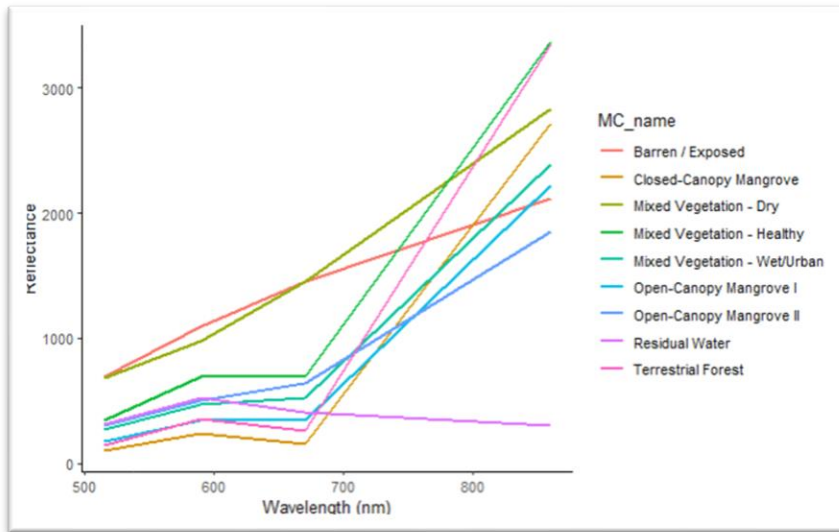


Figure 7 - The variation of spectral separability of all target classes as represented by CRAs across PlanetScope Blue (455-515 nm), Green (500 - 590 nm), Blue (590 - 670 nm), and NIR (780 - 860 nm) bands (Planet, 2023). The set of lines shows the mean reflectance.

2.3 Classification

There are numerous established algorithms for classifying Landsat data to generate maps of mangrove distribution, such as classification and regression trees (CART), support vector machines (SVM), unsupervised k-means, decision trees, and maximum likelihood (ML) (Yancho et al., 2020). For this study, random forest (RF) and maximum likelihood (ML) are used to do the supervised classification, and the algorithm with better output and higher accuracy is kept. RF and ML are both outstanding and well-established classification algorithm that is capable of providing classification with high accuracy (Breiman, 2001; Asmala, A., 2012), and it had been used widely and successfully in a lot of previous mangroves research (Yancho et al., 2020; Rogers et al., 2017; Jones et al., 2016). The classification took place on R software with input of 70% of the training dataset. The dataset includes the CRAs and the derived spectral indices from section 2.1, and the base map is the map at corresponding year acquired in Module 1. The output is composed of only one band with each pixel assigned the value of the classified landcover index.

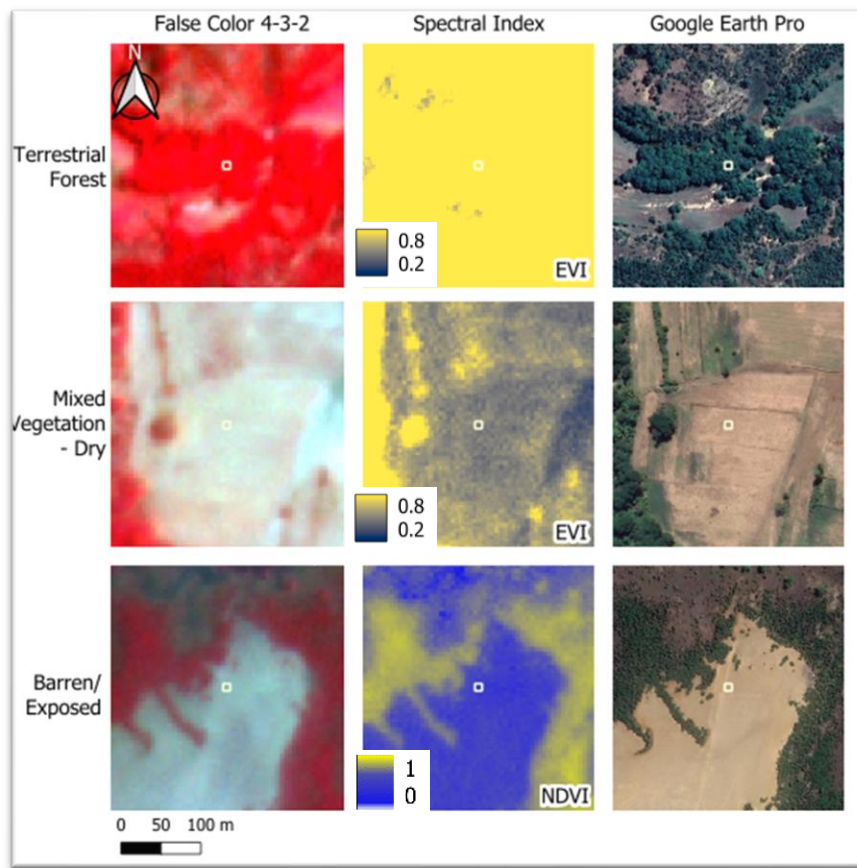
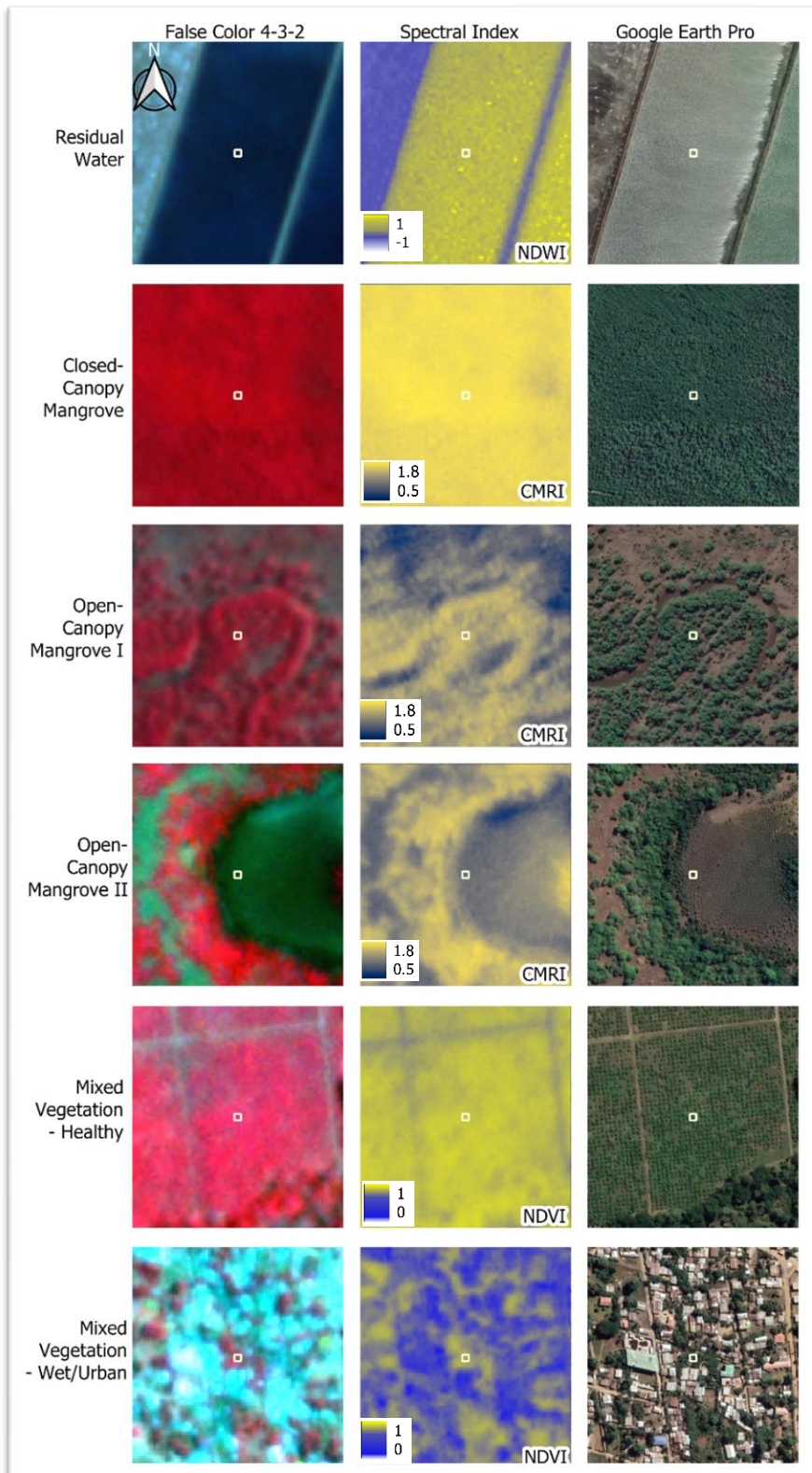


Figure 8 – The appearance of all targeted classes of full classification in 3m pixel PlanetScope Imagery acquired from Planet data in August 2022, and fine spatial resolution satellite imagery accessible in Google Earth Pro (Google, Mountain View, CA, USA). The False color composite 4-3-2 are shown in R-NIR, G-Red, B-Green. For Spectral Indices, Enhanced Vegetation Index (EVI-Matsushita et al., 2007), Normalized Difference Vegetation Index (NDVI-Gandhi et al., 2015), Normalized Difference Water Index (NDWI-McFeeters, 2013), Combined Mangrove Recognition Index (CMRI-Gupta et al., 2018) are used

Figure 8 cont.



2.4 Accuracy Assessment

The substitution and error matrices of all output classifications will be produced by the method used by Rosenfield on R (Rosenfield, 1986). The resubstituting matrices determine the final land-cover class for the CRAs that were used to train the classifier (Rosenfield, 1986). The error matrices utilize 30% of CRAs withheld from categorization to test the accuracy of maps independently (Rosenfield, 1986). The confusion matrix includes Producer's Accuracy (PA) on the bottom row, the User's Accuracy on the rightmost column, and Overall Accuracy (OA) printed below the table. The output of this module consists of (1) full and binary classification maps in 2022, (2) a confusion matrix of full and binary classification in 2020 and 2022, and a corresponding accuracy assessment.

Module 3 – Dynamics and comparison with GEM result

Multi-date outputs of PlanetScope data are used to quantify dynamics. This is foundational to understanding long-term trends and the effectiveness of conservation efforts (Yancho et al., 2020). Also, a 1:8000 scaled classified map based on Planet data and Landsat data is used to show the advanced details included in the fine spatial resolution map. The “true mangrove” (closed canopy mangrove and open canopy mangrove I) extent obtained by the binary classification of PlanetScope data in 2020 and GEM data in 2020 is also graphed. The output of this module includes (1) the dynamic of mangrove extent based on multi-date maps (2) a comparison between GEM maps and PlanetScope maps (3) a comparison of the “true mangrove” extent identified by Planet map and GEM map in the same year.

4. Result

Module 1 – Defining the Area of Interest (AOI) and Compositing Imagery

Two masked multi-date maps of 2020 and 2022 composed of PlanetScope Imagery with 3.0 m pixel size and 4 bands – Blue, Green, Red, NIR, are generated and used as input for classification in Module 2.

Module 2 – Classification Reference Areas (CRAs), Spectral Separability, Classifications, and Accuracy Assessment

(1) Full and binary classification maps in 2022

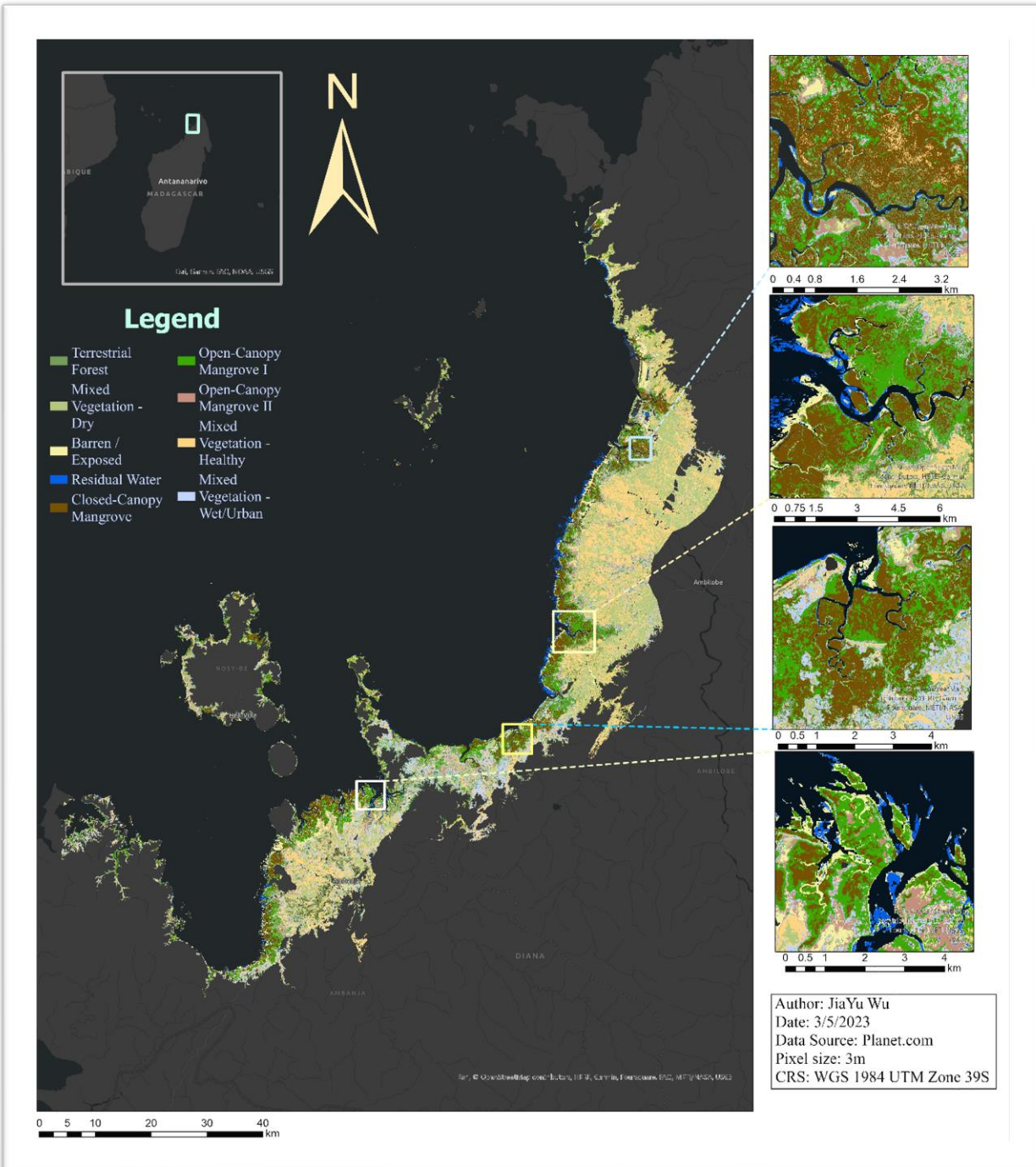


Figure 9 - The Full Classification Map of Nine Mangrove Subtypes in TAB in 2022; The four focused maps are coastal streams with high mangrove densities to show the advanced details of the map

Figure 9 is generated by the Maximum Likelihood Classification Algorithm by R with a relatively high accuracy of over 91% and kappa of 0.8684. The inset maps show the mangrove cover in four main coastal streams in AOI.

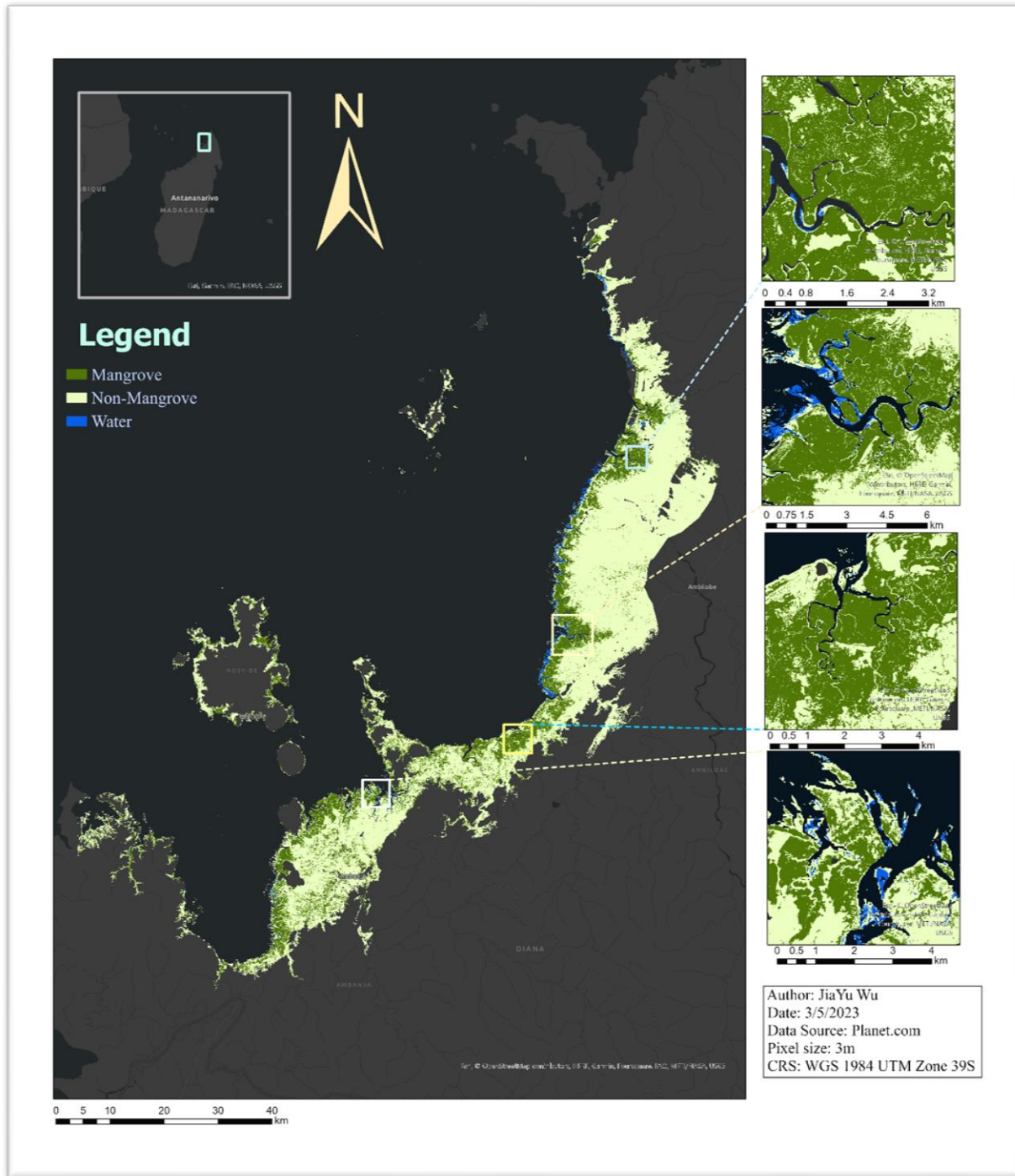


Figure 10 - The Binary Classification Map of Mangrove Covers in TAB in 2022; The four focused maps are coastal streams with high mangrove densities to show the advanced details of the map

Figure 10 is generated by the Maximum Likelihood Classification Algorithm by R with a relatively high accuracy of 90% and kappa of 0.8057. The inset maps show the mangrove cover in four main coastal streams in AOI. Overall, the result is meaningful and can be useful to update the current extent of subtypes of mangroves.

(2) Accuracy assessment.

	Terrestrial Forest	Mixed Vegetation - Dry	Barren / Exposed	Residual Water	Closed-Canopy Mangrove	Open-Canopy Mangrove I	Open-Canopy Mangrove II	Mixed Vegetation - Healthy	Mixed Vegetation-Wet/Urban	Total
Terrestrial Forest	53	0	0	0	15	0	0	0	0	68
Mixed Vegetation - Dry	0	47	6	0	0	0	0	0	0	53
Barren / Exposed	0	0	75	0	0	0	0	0	0	75
Residual Water	0	0	0	27	0	0	0	0	0	27
Closed-Canopy Mangrove	1	0	0	0	247	0	0	0	0	248
Open-Canopy Mangrove I	0	0	0	0	6	65	0	0	6	77
Open-Canopy Mangrove II	0	0	0	0	0	0	43	0	7	50
Mixed Vegetation - Healthy	3	0	0	0	0	0	0	36	7	46
Mixed Vegetation -Wet/Urban	3	0	0	0	0	0	0	9	50	62
Total	60	47	81	27	268	65	43	45	70	706

Table 5 - The Confusion Matrix of the full classification of mangroves at TAB in 2022 based on PlanetScope data

	Terrestrial Forest	Mixed Vegetation - Dry	Barren / Exposed	Residual Water	Closed-Canopy Mangrove	Open-Canopy Mangrove I	Open-Canopy Mangrove II	Mixed Vegetation - Healthy	Mixed Vegetation-Wet/Urban	Total
Terrestrial Forest	54	0	0	0	0	4	0	0	0	58
Mixed Vegetation - Dry	0	44	0	0	0	0	0	0	0	44
Barren / Exposed	0	2	73	0	0	0	0	0	1	76
Residual Water	0	0	0	26	0	0	0	0	1	27
Closed-Canopy Mangrove	3	0	0	0	236	0	0	0	0	239
Open-Canopy Mangrove I	0	0	0	0	14	62	2	0	20	98
Open-Canopy Mangrove II	0	0	0	0	0	0	25	1	6	32

Mixed Vegetation - Healthy	2	0	0	0	0	0	9	52	0	63
Mixed Vegetation - Wet/Urban	0	0	6	0	9	5	6	8	46	80
Total	59	46	79	26	259	71	42	61	74	717

Table 6 - The Confusion Matrix of the full classification of mangroves at TAB in 2020 based on PlanetScope data

		2022		2020	
		PA	UA	PA	UA
Terrestrial Forest		88.33%	77.94%	91.53%	93.10%
Mixed Vegetation - Dry		100.00%	88.68%	95.65%	100.00%
Barren / Exposed		92.59%	100.00%	92.41%	96.05%
Residual Water		100.00%	100.00%	100.00%	96.30%
Closed-Canopy Mangrove		92.16%	99.60%	91.12%	98.74%
Open-Canopy Mangrove I		100.00%	84.42%	87.32%	63.27%
Open-Canopy Mangrove II		100.00%	86.00%	59.52%	78.12%
Mixed Vegetation - Healthy		80.00%	78.26%	85.25%	82.54%
Mixed Vegetation - Wet/Urban		71.43%	80.65%	62.16%	57.50%
Overall Accuracy		91.07%		86.19%	
Kappa		0.8684		0.8318	

Table 7 - The PA (Producer's Accuracy), UA (User's Accuracy), and Overall Accuracy and Kappa of the full classification of mangroves at TAB in 2020 and 2022 based on PlanetScope data

	Mangrove	Non-Mangrove	Water	Total
Mangrove	339	38	0	377
Non-Mangrove	24	316	14	354
Water	0	0	13	13
Total	363	354	27	744

Table 8 - The Confusion Matrix of the binary classification of mangroves at TAB in 2022 based on PlanetScope data with Producer's Accuracy (PA) and User's Accuracy (UA)

	Mangrove	Non-Mangrove	Water	Total
Mangrove	467	38	0	505
Non-Mangrove	43	425	5	473
Water	0	1	55	56
Total	510	464	60	1034

Table 9 - The Confusion Matrix of the binary classification of mangroves at TAB in 2020 based on PlanetScope data with Producer's Accuracy (PA) and User's Accuracy (UA)

		2022		2020	
		PA	UA	PA	UA
Mangrove		93%	90%	91.57%	92.48%
Non-Mangrove		89%	89%	91.59%	89.85%
Water		48%	100%	91.67%	98.21%
Overall Accuracy		89.78%		91.59%	
Kappa		0.8057		0.8512	

Table 10 - The PA (Producer's Accuracy), UA (User's Accuracy), and Overall Accuracy and Kappa of the Binary classification of mangroves at TAB in 2020 and 2022 based on PlanetScope data

From Table 7 and Table 10, we can see that the accuracy assessment is relatively high, especially for the classes that we are most interested in, which are Closed-Canopy Mangrove, Open-Canopy Mangrove I, and Open-Canopy Mangrove II.

Module 3 – Dynamics and comparison with GEM result

(1) The dynamic of mangrove extent based on multi-date maps

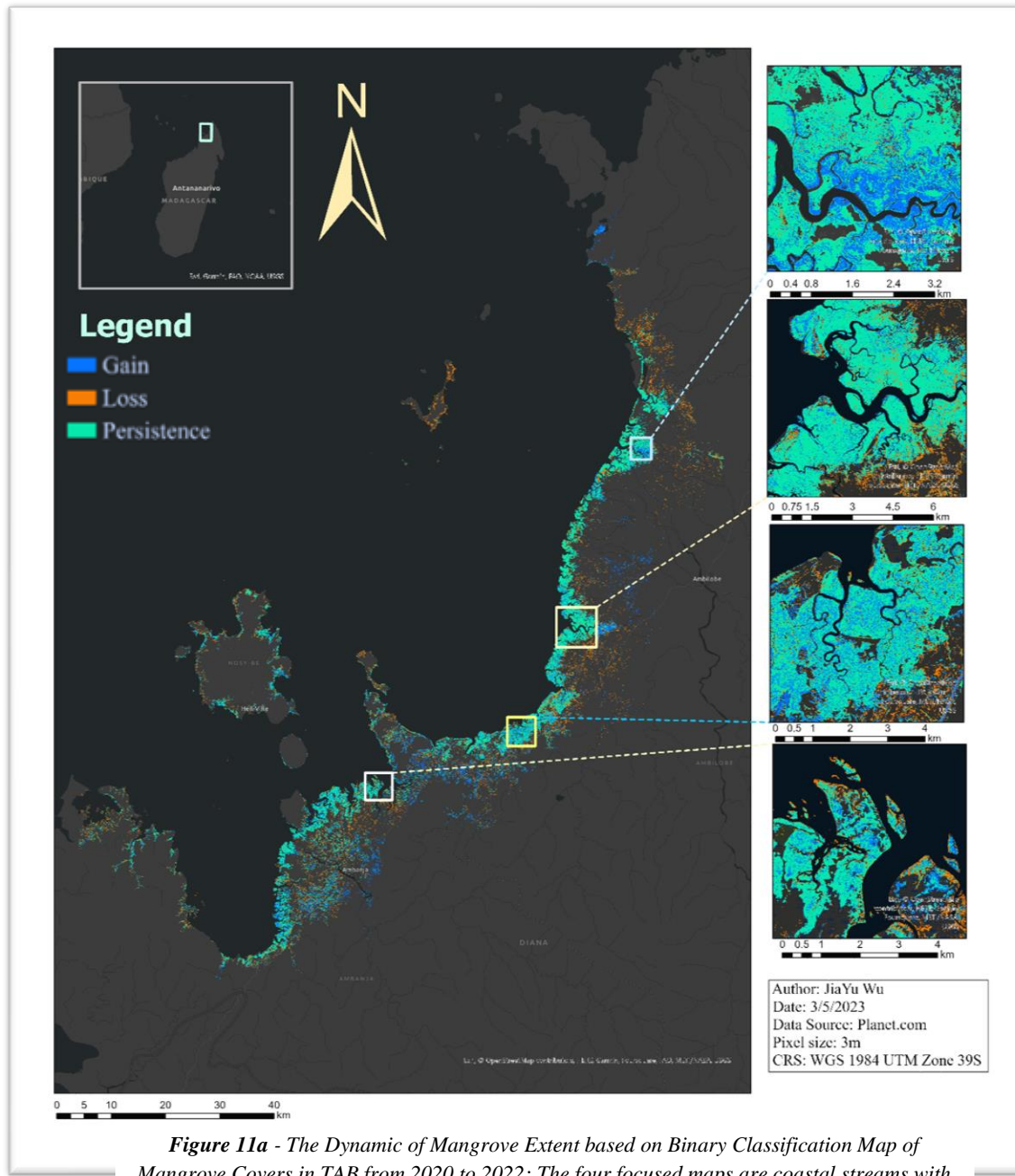


Figure 11a - The Dynamic of Mangrove Extent based on Binary Classification Map of Mangrove Covers in TAB from 2020 to 2022; The four focused maps are coastal streams with high mangrove densities to show the advanced details of the map

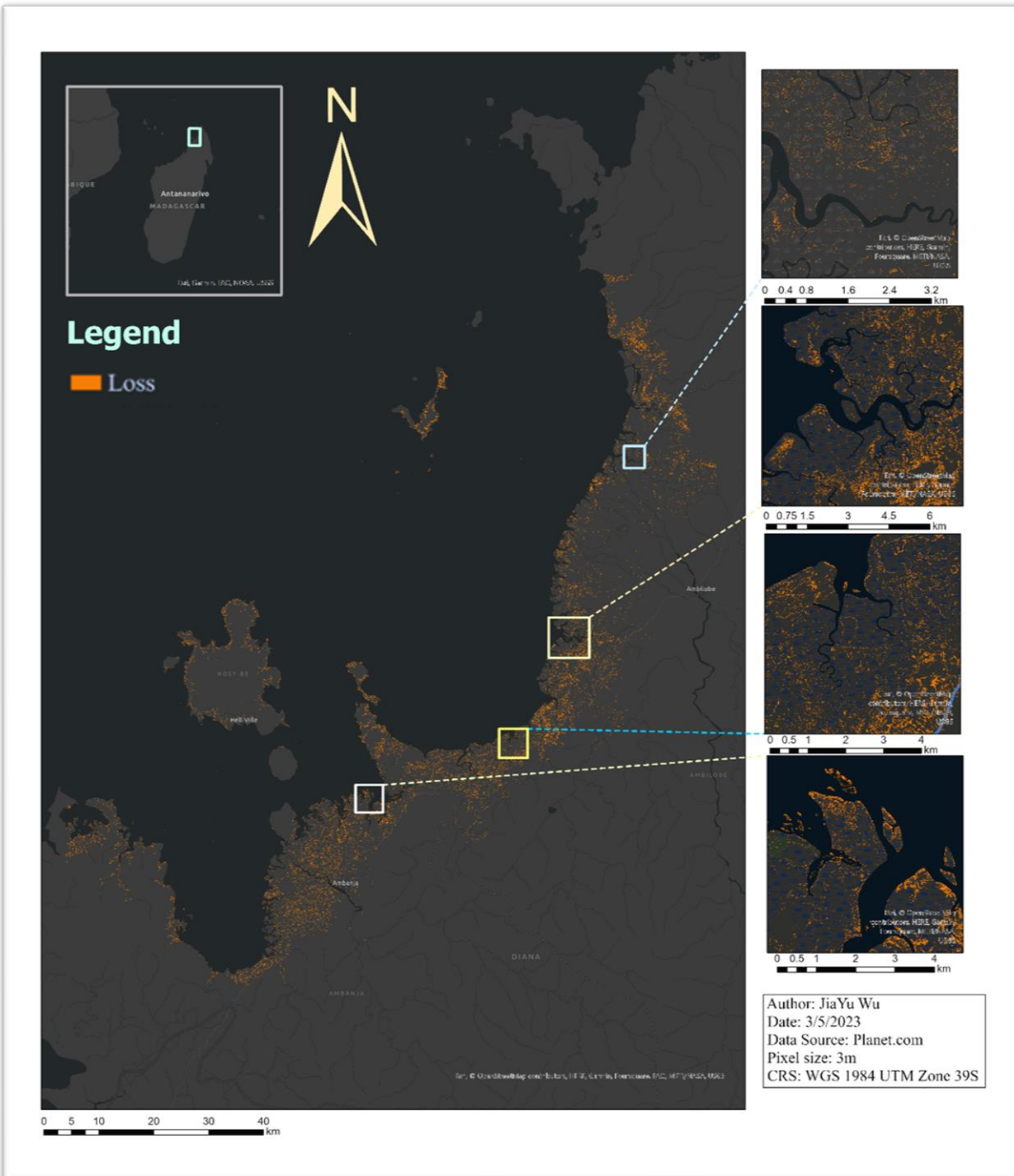


Figure 11b - The Loss of Mangrove Extent based on Binary Classification Map of Mangrove Covers in TAB from 2020 to 2022; The four focused maps are coastal streams with high mangrove densities to show the advanced details of the map

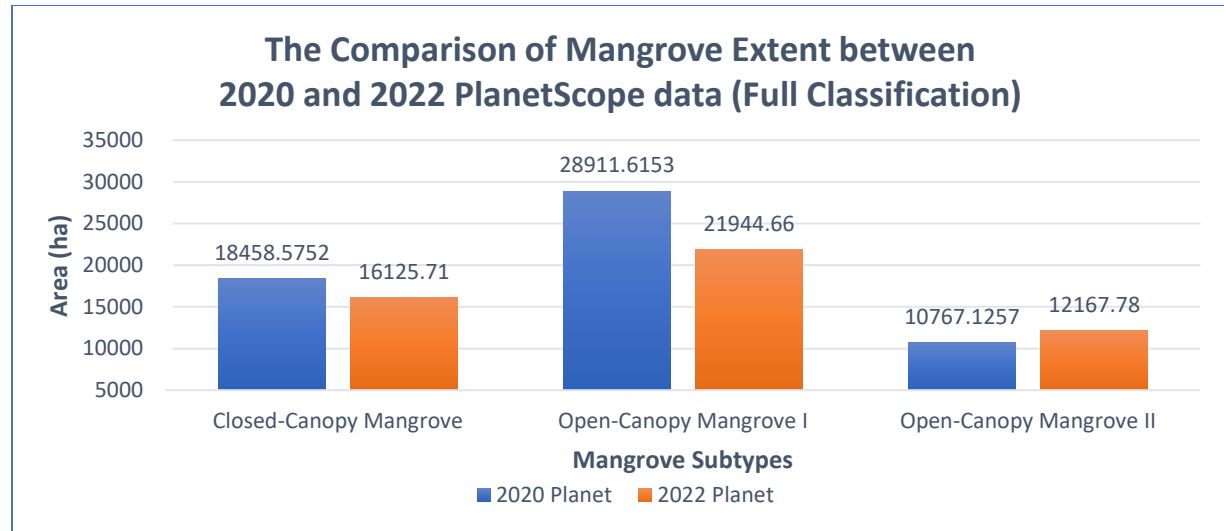


Figure 12 - The Dynamic of Mangrove Extent based on Full Classification Map of Mangrove Covers in TAB from 2020 to 2022

Figure 11a and Figure 11b shows the region where the mangrove is gained, lost, or persisted from 2020 to 2022. The inset maps show the dynamic of mangrove cover in four main coastal streams in AOI. Figure 12 shows the dynamic of total mangrove extent in the AOI from 2020 to 2022 including all three mangrove subtypes. Closed-Canopy Mangrove and Open-Canopy Mangrove I shows a trend of significant decreasing through time for around 9,700 ha in total, while Open-Canopy Mangrove II increased for 1400 ha.

(2) Comparison between GEM maps and PlanetScope maps

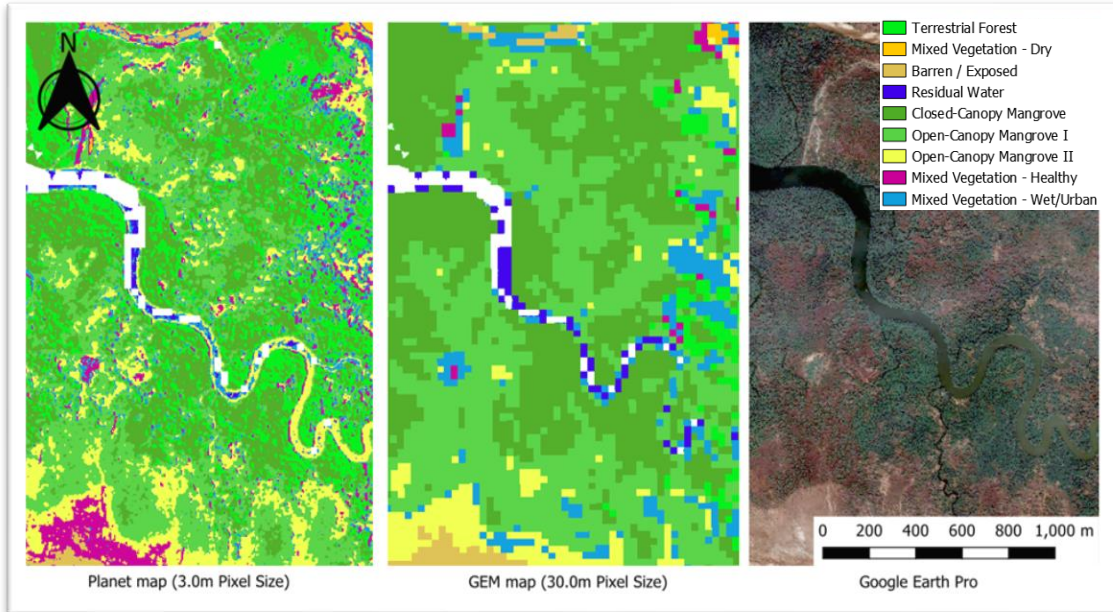


Figure 13 – **Left** - The Full Classification Map of TAB in 2020 based on Planet data; **Middle** - The Full Classification Map of TAB in 2020 generated by GEM; **Right** – fine spatial resolution satellite imagery accessible in Google Earth Pro (Google, Mountain View, CA, USA)

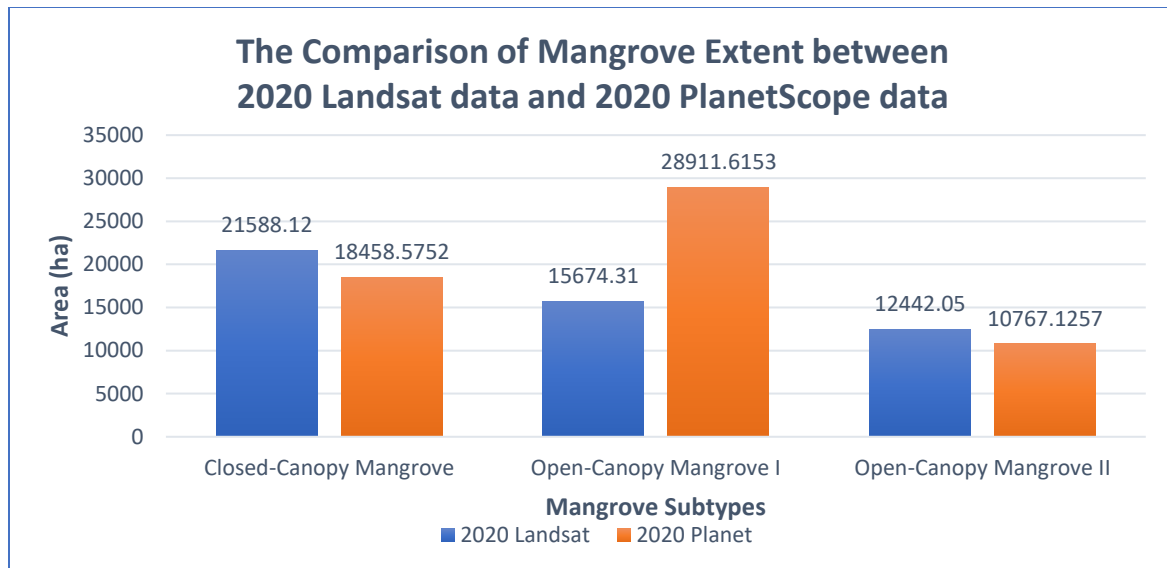


Figure 14 – The Comparison of Mangrove Extent between 2020 Landsat data and 2020 PlanetScope data

Figure 13 shows the advanced detail level provided by the 2020 PlanetScope data comparing to the Landsat data. Figure 14 illustrates that even though they are mapping the same AOI during the same year, the variation is significant. Planet maps indicates a 3000 less hectares cover of Closed-Canopy Mangrove, and a 1500 hectare less Open-Canopy Mangrove II. However, it shows more Open-Canopy Mangrove I coverage of almost 13,000 hectares, which strongly implied that overestimation had occurred.

(3) Comparison of the “true mangrove” extent identified by Planet map and GEM map in the same year.

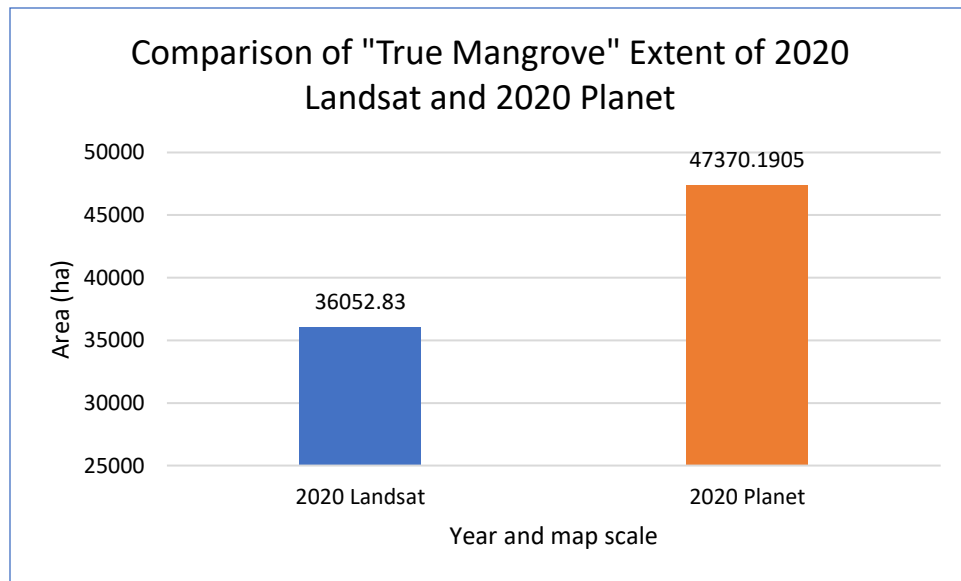


Figure 15 – Comparison of True Mangrove Extent of 2020 Landsat and 2020 PlanetScope; True Mangrove includes Closed-Canopy Mangrove and Open-Canopy Mangrove I, excludes Open-Canopy Mangrove II

From Figure 15, I got that the 2020 Planet map shows over 11,000 hectares more “true mangrove” extent than the GEE map does. Again, implying the presence of overestimation in Open-Canopy Mangrove I in the classification in 2020 Planet map.

5. Discussion

5.1 Brief Summary:

The mangrove subtype distribution in Northwestern Madagascar is successfully identified using Planet data and The Google Earth Engine Mangrove Mapping (GEEMMM). The supervised classification maps of the AOI in 2020 and 2022 are generated with high overall accuracies. Fine resolution data could be used for mangrove/landcover classification, which can identify the exact extent and distribution of different mangrove subtypes. However, limitations that can strongly interrupt the interpretation of the result have to be solved before it can be implemented for practical use. The classification maps have shown a major overestimation issue of Open-Canopy Mangrove I which is the mangrove with short-medium stands and 30-60% closed canopy (Yancho et al., 2020), while restriction is especially obvious in the 2020 map. The PlanetScope based classification result identified nearly one time larger Open-Canopy Mangrove I coverage than the Landsat map does in 2020. This overestimation prevents us from correctly interpret the accurate number of mangroves in the AOI, and it also caused the mangrove loss from 2020 to 2022 to be overestimated. Finally, a higher determination of mangrove extent may mislead local natural resource management teams, leading to inappropriate policies being made.

Until now, most mangrove classification were based on Landsat data and have proven that Landsat imagery can complete the task effective and accurately (Alsaadieh et al., 2013; Long & Giri, 2011; Yancho et al., 2020). But this study provides a more detailed and accurate view of the mangrove cover in the AOI by implementing the Planet data with 10 times smaller pixel size than Landsat does. Overall, the findings of the study provide valuable insights into the changes and trends of mangrove cover in the AOI, while illustrates the potential of using fine resolution satellite imagery data to run the classification.

5.2 Comparison with GEEMMM and limitations:

Landcover classification ran on fine spatial resolution maps are relatively new and challenging compared to the sophisticated and well-developed models ran on Landsat data. Different choice of spatial data could lead to significantly different classification process and outcome, and the difference between GEEMMM and planet are discussed below along with the corresponding limitations.

5.2.1 Classification process

	Planet	GEEMMM
Data Source	PlanetScope	Landsat
Pixel Size	3m	30m

Bands Collected	Visible lights, NIR	Visible lights, NIR, SWIR1, SWIR2
Spectral Index	NDVI, NDWI, EVI, SAVI, OSAVI, CMRI	NDVI, NDWI, MNDWI, SAVI, OSAVI, EVI, LSWI, NDTI, ESBI, CMRI, MMRI, MRI, SMRI
Base map seamline issue	Yes	No

Table 11 – The Comparison of the mangrove classification map based on Planet data and the GEEMMM tool. The bold Index is the mangrove-specific spectral Index (Yancho et al., 2020)

First, GEEMMM used Landsat-8 data which includes the SWIR1 and SWIR2 bands, which are extremely useful in classifying non-forest vegetation (Yancho et al., 2020). The PlanetScope instruments can't record the wavelength of SWIR, causing the limits of spectral index available in this study and increasing the difficulty of deriving the accurate CRAs (Planet, 2023). Moreover, according to the confusion matrix of the 2020 Planet map in Table 5, Open-Canopy Mangrove I is mostly confused with wet/urban vegetation and other mangroves. In GEEMMM, MNDWI, SWIR1, and SWIR2 are believed to be the most useful classifier of open-canopy mangroves (Yancho et al., 2020). However, those three bands are not available in this study, making it hard to clearly identify the cover of mixed vegetation and mangroves, especially for the map in 2020. In GEEMMM, MNDWI, unavailable for Planet, is used for separation from forests and mangroves (Yancho et al., 2020). The relatively poor difference between NIR reflectance is the main classifier used to differentiate between terrestrial forests and closed-canopy mangroves. Either field work or extra fine-resolution spectral data is needed to be used to define the clear boundary between those landcover subtypes and mangrove subtypes. Residual Water is easily distinguished from all other classes by NIR; however, it's sometimes confused with the mud near the coast and misclassified as wet vegetation.

Secondly, the fine spatial resolution planet map restricted its temporal and spatial accessibility compared to the GEEMMM. After applying a strict cloud mask of 30% during data collection in Planet Explorer, the available satellite imagery within the AOI is further restricted, while the PlanetScope imagery is all separated into small pieces that need to be mosaiced together. Finally, the final multi-date base map is assembled by over 100 raster files from multiple months from June to September. This data shortage extends the time of data collection and causes the failure of generating the multi-date map for 2016 as planned in the original research proposal. Most importantly, during the mosaic process, the imagery needs to be taken in a very similar condition, i.e., same time of day, sun elevation, off-nadir angle, sun azimuth, and ground sample distance, to guarantee the smooth transition between two pieces of imagery. However, due to data shortage, it's extremely hard to make sure all the transitions are smooth, and no seamline issues are raised. This seamline caused the sudden gap in index values within the base map, which leads to the misclassification in the result like the result in Figure 16. The eastern side of the seamline is all expected to be closed-canopy mangrove, but they are all misclassified as Open-Canopy mangrove I, leading to the variation of underestimating closed-canopy mangrove extent and overestimating open-canopy mangrove I extent for the planet map 2020.

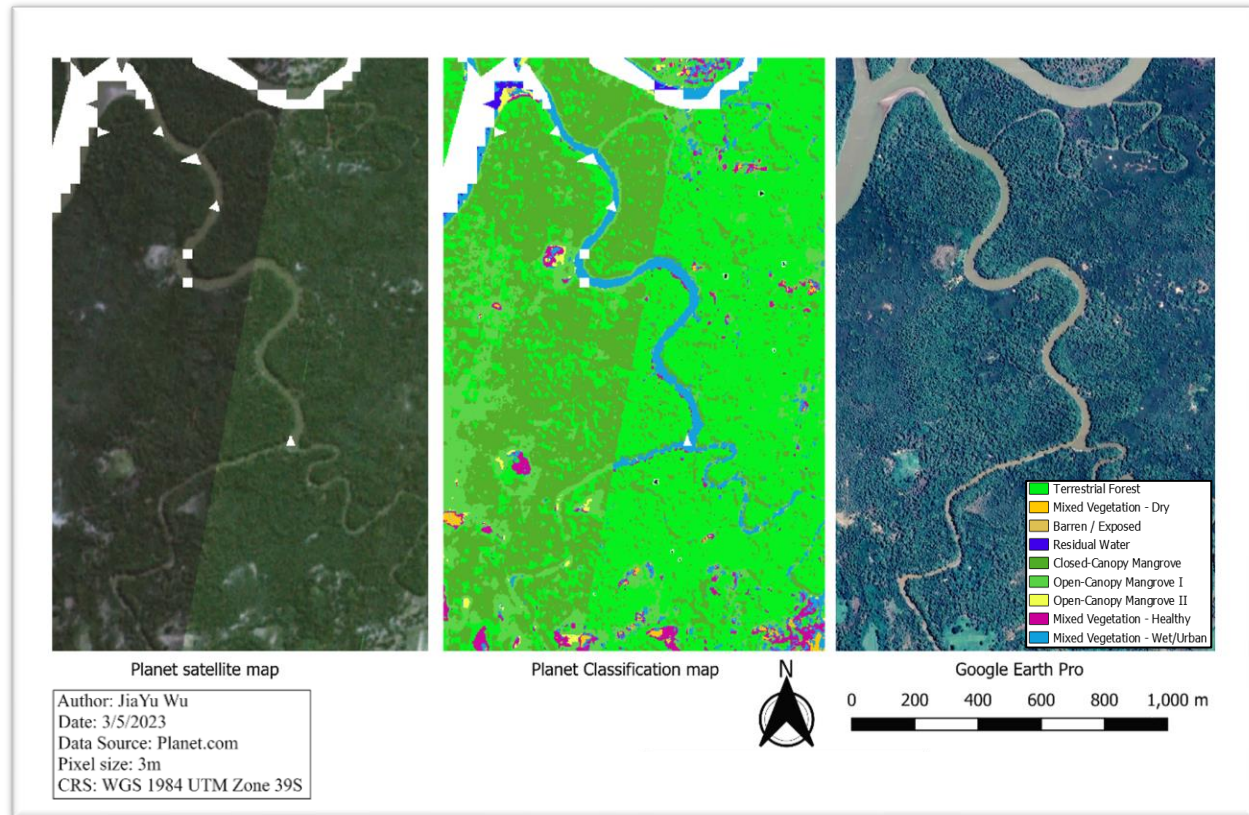


Figure 16 – Left - The Satellite map of TAB in 2020 based on Planet data; **Middle** - The Full Classification Map of TAB in 2020 based on Planet data; **Right** – fine spatial resolution satellite imagery accessible in Google Earth Pro (Google, Mountain View, CA, USA)

5.2.2 Classification result

5.2.2.1 Shadow misclassification

Since the most updated GEEMMM classification map is in 2020, the full and binary classification maps of Planet 2020 and GEEMMM 2020 are compared directly with each other. Figure 15 illustrates that the variation is significant even though they are mapping the same AOI during the same year. The different mangrove extent is not only caused by the value gap due to the seamline in the Planet map but also caused by the confusion between the terrestrial forest shadow and the mangrove as shown in Figure 17 below. It overestimates the cover of Open-Canopy mangrove I for both the full and binary classification results for the planet map. Moreover, typically binary classification generates a higher accuracy than the full classification does (Brownlee, 2020). But in this study, the accuracy assessment shows that the binary and the full classification have similar accuracy, and this shadow misclassification issue is the main driver of this similarity. After careful interpretation, this issue is also found in the Landsat classification maps, however, the relatively coarse spatial resolution helps in weakening the error since the shadows are usually smaller than the size of a single pixel. The refined resolution of the

planet map exaggerates the problem and causes a major distinction in the result of the mangrove-covered area.

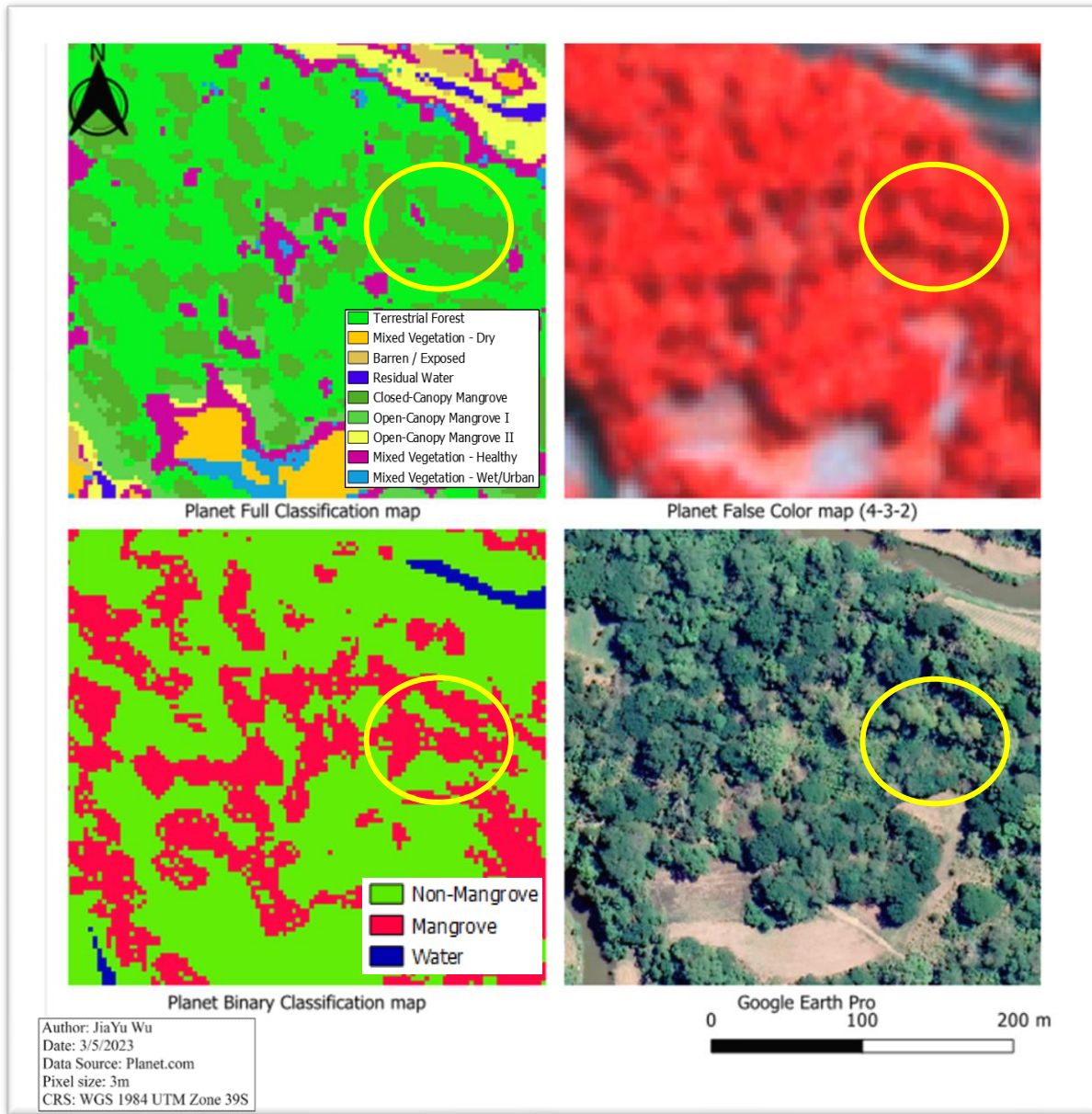


Figure 17 – Top Left – The Full Classification Map of TAB in 2020 based on Planet data; **Top Right** – The False color composite of Planet 2020 map with 4-3-2 as R-NIR, G-Red, B-Green; **Bottom Left** – The Binary Classification Map of TAB in 2020 based on Planet data; **Bottom Right** – fine spatial resolution satellite imagery accessible in Google Earth Pro (Google, Mountain View, CA, USA); Yellow circle indicates an example of confusion between shadows and mangroves

5.2.2.2 Approaches taken to solve the misclassification

After recognizing this issue during the process of refining my model, a few new approaches are tried to solve this issue including adding an extra landcover class of shadow and deriving corresponding CRAs. This approach doesn't work properly with poor accuracy

outcomes of nearly <70% overall accuracy, and PA and UA also drop for the mangrove classes and forests. Another approach I tried is to enlarge my sample size, i.e., acquire more data for training/validation, which is proved to be a reliable way to refine a classification model (Verma, 2022). However, the dataset seems to be unbalanced after doubling the total sample size from 200 to 400, which means that it's unable to contribute to a better accuracy result or it failed to add more samples to some of the landcover classes.

5.3 Possible Improvements and future directions:

There are a few ways that may help in creating a more accurate supervised classification model than this study does. Firstly, the only classification algorithms used in this project are Random Forest and maximum likelihood (Breiman, 2001; Asmala, A., 2012). There are other sophisticated and established algorithms that had been used in previous mangrove distribution analyses based on Landsat but not tested in this study, including regression trees (CART), support vector machines (SVM), unsupervised k-mean, and decision trees (Zhang et al., 2017; Xia et al., 2018; Mondal et al., 2017; Yancho et al., 2020). Also, the procedure of data collection of fine-resolution satellite images needs to be improved by eliminating the value gaps and guaranteeing smoothness and uniformity throughout the map. Moreover, using satellite image is not the only way to identify the mangrove extent. Other remote sensing approaches like LiDAR can also provide valuable and effective mangrove species classification (Cao et al., 2018).

Reference

Alsaideh, B., Al-Hanbali, A., Tateishi, R., Kobayashi, T., & Hoan, N. T. (2013). Mangrove forests mapping in the southern part of Japan using landsat ETM+ with Dem. *Journal of Geographic Information System*, 05(04), 369–377. <https://doi.org/10.4236/jgis.2013.54035>

Arias-Ortiz, A., Masqué, P., Glass, L., Benson, L., Kennedy, H., Duarte, C. M., Garcia-Orellana, J., Benitez-Nelson, C. R., Humphries, M. S., Ratefinjanahary, I., Ravelonjatovo, J., & Lovelock, C. E. (2020). Losses of soil organic carbon with deforestation in mangroves of Madagascar. *Ecosystems*, 24(1), 1–19. <https://doi.org/10.1007/s10021-020-00500-z>

Asmala, A. (2012). Analysis of Maximum Likelihood Classificationon Multispectral Data.

Benson, L., Glass, L., Jones, T., Ravaoarinorotsihoarana, L., & Rakotomahazo, C. (2017). Mangrove carbon stocks and ecosystem cover dynamics in southwest Madagascar and the implications for Local Management. *Forests*, 8(6), 190. <https://doi.org/10.3390/f8060190>

Breiman, L. (2001). Random Forest. *Machine Learning*, 45(1), 5–32. <https://doi.org/10.1023/a:1010933404324>

Brownlee, J. (2020, August 19). 4 types of classification tasks in machine learning. MachineLearningMastery.com. Retrieved March 20, 2023, from [https://machinelearningmastery.com/types-of-classification-in-machine-learning/#:~:text=Binary%20classification%20refers%20to%20those,prediction%20\(churn%20or%20not\).](https://machinelearningmastery.com/types-of-classification-in-machine-learning/#:~:text=Binary%20classification%20refers%20to%20those,prediction%20(churn%20or%20not).)

Cao, J., Leng, W., Liu, K., Liu, L., He, Z., & Zhu, Y. (2018). Object-based mangrove species classification using unmanned aerial vehicle hyperspectral images and Digital Surface Models. *Remote Sensing*, 10(2), 89. <https://doi.org/10.3390/rs10010089>

Fern, R. R., Foxley, E. A., Bruno, A., & Morrison, M. L. (2018). Suitability of NDVI and osavi as estimators of green biomass and coverage in a semi-arid rangeland. *Ecological Indicators*, 94, 16–21. <https://doi.org/10.1016/j.ecolind.2018.06.029>

Gandhi, G. M., Parthiban, S., Thummalu, N., & Christy, A. (2015). NDVI: Vegetation change detection using remote sensing and GIS – A case study of vellore district. *Procedia Computer Science*, 57, 1199–1210. <https://doi.org/10.1016/j.procs.2015.07.415>

Gao, B.-cai. (1996). Ndwi—a normalized difference water index for remote sensing of vegetation liquid water from space. *Remote Sensing of Environment*, 58(3), 257–266. [https://doi.org/10.1016/s0034-4257\(96\)00067-3](https://doi.org/10.1016/s0034-4257(96)00067-3)

Google Earth Pro; Google LLC: Mountain View, CA, USA, 2022.

Gupta, K., Mukhopadhyay, A., Giri, S., Chanda, A., Datta Majumdar, S., Samanta, S., Mitra, D., Samal, R. N., Pattnaik, A. K., & Hazra, S. (2018). An index for discrimination of mangroves from non-mangroves using Landsat 8 Oli imagery. *MethodsX*, 5, 1129–1139. <https://doi.org/10.1016/j.mex.2018.09.011>

Huete, A. R. (1988). A soil-adjusted vegetation index (SAVI). *Remote Sensing of Environment*, 25(3), 295–309. [https://doi.org/10.1016/0034-4257\(88\)90106-x](https://doi.org/10.1016/0034-4257(88)90106-x)

Jones, T. G., Ratsimba, H. R., Carro, A., Ravaoarinorotsihoarana, L., Glass, L., Teoh, M., Benson, L., Cripps, G., Giri, C., Zafindrasilivonona, B., Raherindray, R., Andriamahenina, Z., & Andriamahefazafy, M. (2016). The mangroves of Ambanja and Ambaro Bays, northwest madagascar: Historical Dynamics, current status and deforestation mitigation strategy. *Estuaries of the World*, 67–85. https://doi.org/10.1007/978-3-319-25370-1_5

Jones, T., Glass, L., Gandhi, S., Ravaoarinorotsihoarana, L., Carro, A., Benson, L., Ratsimba, H., et al. (2016). Madagascar's Mangroves: Quantifying Nation-Wide and Ecosystem Specific Dynamics, and Detailed Contemporary Mapping of Distinct Ecosystems. *Remote Sensing*, 8(2), 106. MDPI AG. Retrieved from <http://dx.doi.org/10.3390/rs8020106>

Jones, T., Ratsimba, H., Ravaoarinorotsihoarana, L., Cripps, G., & Bey, A. (2014). Ecological Variability and Carbon Stock Estimates of Mangrove Ecosystems in Northwestern Madagascar. *Forests*, 5(1), 177–205. MDPI AG. Retrieved from <http://dx.doi.org/10.3390/f5010177>

Jones, T., Ratsimba, H., Ravaoarinorotsihoarana, L., Glass, L., Benson, L., Teoh, M., Carro, A., Cripps, G., Giri, C., Gandhi, S., Andriamahenina, Z., Rakotomanana, R., & Roy, P.-F. (2015). The dynamics, ecological variability and estimated carbon stocks of mangroves in Mahajamba Bay, Madagascar. *Journal of Marine Science and Engineering*, 3(3), 793–820. <https://doi.org/10.3390/jmse3030793>

Long, J. B., & Giri, C. (2011). Mapping the Philippines' mangrove forests using landsat imagery. *Sensors*, 11(3), 2972–2981. <https://doi.org/10.3390/s110302972>

Matsushita, B., Yang, W., Chen, J., Onda, Y., & Qiu, G. (2007). Sensitivity of the enhanced vegetation index (EVI) and Normalized Difference Vegetation Index (NDVI) to topographic effects: A case study in high-density Cypress Forest. *Sensors*, 7(11), 2636–2651. <https://doi.org/10.3390/s7112636>

McFeeters, S. (2013). Using the normalized difference water index (NDWI) within a geographic information system to detect swimming pools for mosquito abatement: A practical approach. *Remote Sensing*, 5(7), 3544–3561. <https://doi.org/10.3390/rs5073544>

Mondal, P., Trzaska, S., & de Sherbinin, A. (2017). Landsat-derived estimates of mangrove extents in the Sierra Leone Coastal Landscape Complex during 1990–2016. *Sensors*, 18(2), 12. <https://doi.org/10.3390/s18010012>

Planet. (2022). PlanetScope. Planetscope. Retrieved October 28, 2022, from <https://developers.planet.com/docs/data/planetscope/>

Planet. (2023). Understanding planetscope instruments. Retrieved March 6, 2023, from <https://developers.planet.com/docs/apis/data/sensors/>

Rogers, K., Lymburner, L., Salum, R., Brooke, B. P., & Woodroffe, C. D. (2017). Mapping of mangrove extent and zonation using high and low tide composites of Landsat Data. *Hydrobiologia*, 803(1), 49–68. <https://doi.org/10.1007/s10750-017-3257-5>

Rosenfield, G. H. (1986). Analysis of thematic map classification error matrices. *Photogrammetric Engineering and Remote Sensing*, 52(5), 681-686.

Wilkie, M. L., & Fortuna, S. (2003). Forest Resources Assessment Working Paper. In Status and trends in mangrove area extent worldwide (pp. 287). essay, Forestry Dept., Food and Agriculture Organization of the United Nations.

World Wildlife Fund. (2022). Madagascar. WWF. Retrieved October 28, 2022, from <https://www.worldwildlife.org/places/madagascar>

Xia, Q., Qin, C.-Z., Li, H., Huang, C., & Su, F.-Z. (2018). Mapping mangrove forests based on multi-tidal high-resolution satellite imagery. *Remote Sensing*, 10(9), 1343. <https://doi.org/10.3390/rs10091343>

Yancho, J., Jones, T., Gandhi, S., Ferster, C., Lin, A., & Glass, L. (2020). The Google Earth Engine Mangrove Mapping Methodology (GEEMMM). *Remote Sensing*, 12(22), 3758. <https://doi.org/10.3390/rs12223758>

Yancho, J., Jones, T., Gandhi, S., Ferster, C., Lin, A., & Glass, L. (2020). The Google Earth Engine Mangrove Mapping Methodology (GEEMMM). *Remote Sensing*, 12(22), 3758. MDPI AG. Retrieved from <http://dx.doi.org/10.3390/rs12223758>

Zhang, X., Treitz, P. M., Chen, D., Quan, C., Shi, L., & Li, X. (2017). Mapping mangrove forests using multi-tidal remotely-sensed data and a decision-tree-based procedure.

International Journal of Applied Earth Observation and Geoinformation, 62, 201–214.
<https://doi.org/10.1016/j.jag.2017.06.010>